International Journal of Advances in Engineering and Management (IJAEM)
Volume 7, Issue 05 May 2025, pp: 471-482 www.ijaem.net ISSN: 2395-5252

Unified Thermal Image Enhancement for Object Detection and Visual Clarity

S. Hovhannisyan[1], T. Trongtirakul[2], S. Agaian[3]

[1]*Department of Mathematics and Mechanics, Yerevan State University, Yerevan, 0025, Armenia*
[2] *Department of Electrical Engineering, Faculty of Industrial Education, Rajamangala University of Technology Phra Nakhon, 399 Samsen Rd, Wachira Phayaban, Dusit, Bangkok 10300, Thailand*
[3] *Department of Computer Science, College of Staten Island, 2800 Victory Blvd. Staten Island, New York, NY 10314, USA*

Date of Submission: 15-05-2025 Date of Acceptance: 25-05-2025

ABSTRACT: Thermal infrared imaging systems are increasingly important in autonomous driving, medical diagnostics, and solar panel inspection applications. However, the effectiveness of thermal images is often limited by low contrast, indistinct details, uneven illumination, and various artifacts that hinder human interpretation and automated analysis. Conventional and deep learning-based enhancement methods offer partial solutions but frequently struggle to generalize across diverse conditions or produce consistently high-quality results.

This paper proposes a unified thermal image enhancement pipeline that combines decomposition-based image processing, robust illumination balancing, and analytically designed pseudo-coloring schemes to enhance visual clarity, preserve structural details, and deliver interpretable colorized outputs suited for downstream tasks. Our methodology consists of a three-stage pipeline: (1) decomposition to separate fine details from the base structure, (2) adaptive contrast enhancement using the specialized module, and (3) pseudo-coloring that maps thermal intensities to perceptually meaningful color spaces. The pipeline enhances visual clarity, preserves structural details, and delivers interpretable colorized outputs suited for downstream tasks. Extensive experimentation on multiple real-world datasets, including autonomous vehicles, demonstrates that our method significantly improves visual quality and object detection performance. Furthermore, evaluation of the proposed enhancement and coloring techniques using the YOLOv7 object detector shows that our approach yields up to 2.6% higher $mAP_{0.5}$ compared to models trained on original thermal images, highlighting its effectiveness in improving object detection accuracy.

KEYWORDS: Image decomposition, Object detection, Pseudo-colorization, Thermal image enhancement.

I. INTRODUCTION

RGB camera-based computer vision systems often face significant limitations due to varying lighting conditions and low-light environments. Thermal imaging technology provides a robust alternative, effectively overcoming these drawbacks inherent in standard color imagery. Thermal imaging systems perform well under diverse environmental conditions, capturing temperature information through mid- and long-wavelength infrared bands. This capability is particularly valuable in applications where visual data is unreliable, such as security monitoring [1], autonomous vehicle navigation [2], military surveillance [3], medical diagnostics [4], and UAV-based solar panel inspection systems.

For instance, thermal imaging enhances security systems by reliably detecting intruders under low-visibility conditions. Autonomous vehicles utilize thermal imaging to identify pedestrians, vehicles, and essential traffic infrastructure, significantly improving road safety. In medical diagnostics, thermal imaging supports non-invasive procedures such as breast cancer screening, while UAV-assisted solar panel inspections leverage thermal imaging to identify panel defects. However, thermal imaging often suffers from issues like uneven brightness, including excessively bright or overly dim regions, which limit the clarity of visualized targets and hinder broader infrared application deployment.

Various thermal image enhancement methods have been developed to address these limitations and improve the visibility, clarity, and overall quality of thermal images for automated processing systems. Effective thermal enhancement enhances decision-making and operational safety across numerous domains. Several image improvement and enhancementstrategies have emerged in recent years to address the persistent challenges of low-quality thermal imagery. Broadly, these techniques can be divided into two main categories: traditional methods and learning-based approaches. Traditional algorithms typically focus on adjusting key image parameters, such as contrast, brightness, and denoising, through explicit mathematical models and handcrafted filters, often requiring careful fine-tuning of hyperparameters to adapt to varying conditions. In contrast, learning-based methods leverage data-driven models, particularly deep neural networks, to automatically learn complex mappings for enhancement and restoration from large datasets.

Traditional Methods: Generally, infrared images are characterized by low contrast, low resolution, and blurred details. To solve these issues, traditional methods already used for visible imaging have been adopted to enhance thermal images. Histogram Equalization (HE) is a well-known algorithm that can readily augment contrast [5]. It has been employed either in its basic form or an extended one. For instance, in [6], a multi-objective HE model was proposed to enhance contrast while preserving the brightness of thermal images. Contrast adjustment techniques [6] can significantly improve image visibility, but their effectiveness often diminishes under uneven illumination. Contrast Limited Adaptive Equalization (CLAHE), based on local contrast modification (LCM) [7], it has also been suggested to emphasize subtle, hidden details and modify the contrast enhancement level. Wavelet-based approaches [8] decompose images into frequency bands, allowing for targeted enhancement and noise reduction. Despite their effectiveness, these methods typically require careful parameter tuning and can demand substantial computational resources. Improper settings can also potentially introduce undesirable artifacts. It is important to note that the equalization histogram methods presented typically produce similar results, but their use can amplify noise in the image.

Learning-based Methods: Deep Neural Networks (DNNs) have recently been applied in numerous computer vision applications, including image classification, object detection, and recognition. Recently published methods for image enhancement have utilized DNN architectures to improve the visual quality of both thermal and visible images. [9] presents first attempts to address this issue, which employs a Convolutional Neural Network (CNN) for Super-Resolution. [10] presents DNN for enhancement, aiming to increase the spatial resolution of visible images. While many current methods for enhancing visible images primarily aim to improve the original image's spatial resolution, only a limited number of studies have addressed other factors, like low contrast and blurred edges, specifically in thermal image enhancement. Recent advancements have explored deep learning methods leveraging neural network architectures for automated thermal image enhancement. These methods address noise reduction, contrast enhancement, and detail refinement. Notably, conditional generative adversarial networks (GANs) have effectively enhanced contrast and detail clarity while reducing noise amplification [11, 12]. However, existing techniques such as IE-CGAN [13], AGCCPF [14], BBCNN [15], and AGCWD [16] focus on specific types of degradation under uneven lighting, often leading to unsatisfactory enhancement outcomes with artificial contrast, particularly in complex lighting conditions.

Pseudo-coloring, another critical method, transforms single-channel thermal images into visually interpretable multi-channel outputs, significantly enhancing image interpretability and facilitating downstream analysis tasks. Appropriate colormap selection can improve anomaly visibility and detection accuracy [17]. Although popular, traditional Jet (rainbow) colormaps exhibit non-uniform luminance progression, creating artificial edges and interpretability issues. Recent developments have introduced perceptually uniform colormaps such as Viridis, Plasma, Magma, and Inferno [18], designed using CIELAB/HCL color spaces to ensure uniform brightness transitions and chromatic consistency. Despite their advantages, these palettes sometimes lack the dynamic range to highlight subtle thermal variations. Google's Turbo colormap addresses some limitations with enhanced luminance continuity but may still indicate misleading category boundaries, especially in green-yellow transitions [19]. Parametric probability-density transformations [20] effectively emphasize specific temperature ranges, significantly improving lesion-to-background contrast in medical imagery, but exhibit sensitivity to parameter choices. The Thermal-Rainbow colormap [21] provides an

International Journal of Advances in Engineering and Management (IJAEM)
Volume 7, Issue 05 May 2025, pp: 471-482 www.ijaem.net ISSN: 2395-5252

intuitive "cool-to-warm" color progression, reducing abrupt transitions characteristic of the Jet colormap, although it remains less uniform than sequential palettes.

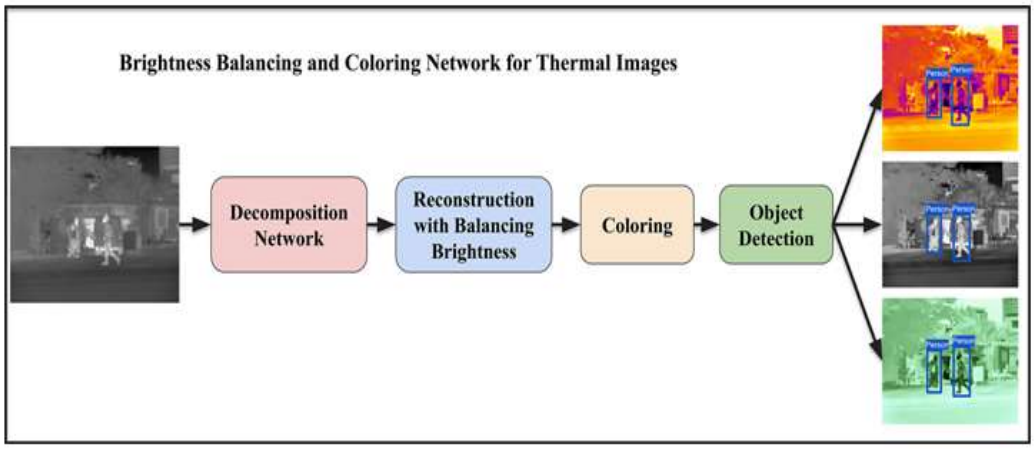

Figure1. Overall architecture of the proposed method

A critical demand remains for simple yet effective thermal enhancement and coloring methodologies. This paper proposes a unified thermal image enhancement pipeline that combines decomposition-based image processing, robust illumination balancing, and analytically designed pseudo-coloring schemes. Our method is designed to maintain high-quality visual outputs suitable for human interpretation and downstream computer vision tasks.

As outlined in the abstract, the proposed pipeline consists of three main stages:

1. **Decomposition and Brightness Balancing**: We adopt an image decomposition method tailored explicitly for thermal imagery. This stage separates fine details from the base structure and introduces a novel brightness balancing and reconstruction technique for thermal infrared images.
2. **Pseudo-Coloring**: We propose two innovative pseudo-coloring approaches:

a. An infrared-based coloring method optimized for robustness in downstream analysis tasks.
b. A light-green coloring approach that enhances visual interpretability for human operators.

3. We validate our proposed method through extensive experiments on three publicly available datasets. We perform thorough evaluations involving image quality metrics and practical object detection scenarios, notably in autonomous driving applications.

II. PROPOSED METHOD

The proposed pipeline is structured as a sequential four-stage processing flow, as shown in Figure 1. The first stage involves decomposing each input thermal image into its constituent reflectance and illumination components using the URetinex-Net framework [22]. URetinex-Net is pre-trained on the LOL low-light dataset after converting all RGB image pairs to grayscale to closely match the statistical characteristics of single-channel thermal data. We maintain the original reflectance-consistency, illumination-smoothness, and perceptual losses as detailed in [22]. This step generates an illumination map as an effective proxy for the scene's temperature distribution, simultaneously isolating essential structural information within the reflectance component.

In the second stage, illumination is balanced using a Residual Channel Attention Network (RCAN) [23], which implements a trainable adaptation of classical histogram equalization [7]. Training pairs are created by applying histogram equalization with randomized clip limits set at 1.2. The network training is supervised using a composite loss function:

$$\mathcal{L}_{\text{RCAN}} = \lambda_{\text{MSE}} \frac{1}{N} \sum_{p} \left(\hat{L}(p) - L_{\text{balanced}}(p) \right)^2 + \lambda_{\text{TV}} |\nabla \hat{L}|_1 \#(1)$$

Here, $\hat{L}$represents the RCAN network output, $\nabla \hat{L}$denotes the discrete gradient operator, and N is the total pixel count. The mean squared

International Journal of Advances in Engineering and Management (IJAEM)
Volume 7, Issue 05 May 2025, pp: 471-482 www.ijaem.net ISSN: 2395-5252

error (MSE) component ensures effective exposure correction, while the total variation (TV) regularization term suppresses small-scale noise that typically results from histogram equalization. The resulting smoothed and balanced illumination $\hat{L}$ is subsequently recombined with the reflectance map R to produce an enhanced grayscale image $\hat{I} = R \cdot \hat{L}$.

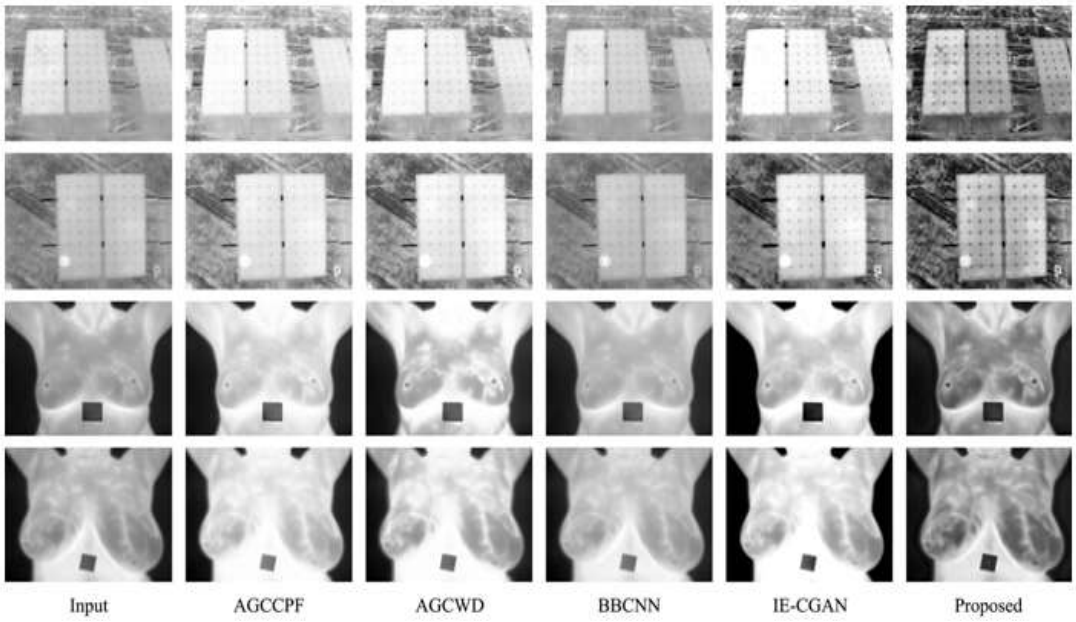

Figure 2. Qualitative comparison of Solar Panel and Breast datasets.

In the third stage, the balanced grayscale image $\hat{I}$undergoes pseudo-coloring, converting single-channel thermal data into visually interpretable three-channel RGB images. For each pixel, the grayscale intensity $g = \hat{I}(x, y) \in \{0, \ldots, 255\}$ is used as an index into predefined analytical functions that produce corresponding RGB values:

$$\mathrm{RGB}(g) = [r(g),\ g(g),\ b(g)]^{T} \#(2)$$

These functions are analytically defined and pre-tabulated into 256-element arrays, as outlined in Table 1, for the infrared and light-green color schemes. The final stage integrates these pseudo-colored images directly into the original three-channel architecture of the YOLOv7 detector [24]. As pseudo-coloring inherently restores the required three-channel input, no further architectural adjustments to YOLOv7 are necessary. The object detector is fine-tuned specifically on the Autonomous Vehicles thermal dataset following the standard YOLOv7 training parameters and loss function, ensuring its effective adaptation to the enhanced and colored images generated by previous stages.

Our proposed method uniquely integrates Retinex-based image decomposition, RCAN-guided illumination balancing, advanced palette-based pseudo-coloring, and a thermal-specific YOLOv7 object detector. This cohesive pipeline effectively normalizes image illumination, enriches visual interpretability through intuitive color mapping, and reliably detects objects under operationally realistic conditions.

III. EXPERIMENTAL RESULTS

This section presents the experimental results of our proposed approach in comparison with several existing methods, including AGCCPF, AGCWD, BBCNN, and IE-CGAN across various datasets, including Autonomous Vehicles [25], Solar Panels [26], and Breast datasets [27]. Through this comparative analysis, we aim to highlight each method's strengths and weaknesses and evaluate the proposed method's effectiveness against these techniques. Moreover, we compare our coloring technique with other widely used coloring methods to highlight its strengths.

QUALITATIVE COMPARISON

Figure 2 compares the enhancement performance of various methods on thermal images from solar panel monitoring and medical imaging datasets. The AGCWD and AGCCPF methods significantly amplify the brightness of already

International Journal of Advances in Engineering and Management (IJAEM)
Volume 7, Issue 05 May 2025, pp: 471-482 www.ijaem.net ISSN: 2395-5252

bright regions, causing critical details in high-temperature areas to become indistinct or lost. This brightness amplification severely limits their usability in practical applications such as precise solar panel fault detection and medical anomaly identification. BBCNN exhibits better stability by uniformly preserving overall contrast across the images, slightly emphasizing defect regions within the solar panels. However, it results in limited visibility improvements, potentially hindering the identification of subtle anomalies. IE-CGAN demonstrates superior performance by selectively enhancing contrast in moderately illuminated regions while controlling overexposure in brighter areas. Our proposed method successfully addresses these limitations by achieving an optimal balance between brightness and contrast enhancement. It distinctly reveals solar panel defects

Table 1. Pseudo-coloring algorithm for infrared and light-green options.

Palette	Channel definition	Constants
Infrared	$r(g) = \begin{cases} Red \\ 0.3217\, g, & g < 20 \\ a \cdot e^{bg} + c \cdot e^{dg}, & g \geq 20 \end{cases}$	a=360.9,b=−0.001182,c=−451.3, d=−0.0134
	$g(g) = \begin{cases} Green \\ 0 \; if \; g < 74 \\ a_0 + \sum_{k=1}^{3} (a_k \cdot cos(k\omega g) + b_k \cdot sin(k\omega g)), \end{cases}$	a_0=95.3,a_1=−100.4,b_1=−74.29, a_2=−5.162,b_2=27.98,a_3=9.364, b_3 =7.937,ω=0.01617
	Blue $b(g) = \sum_{k=1}^{5} a_k \cdot sin(b_k g + c_k)$	a_1=483.1,b_1=0.01307,c_1=−1.157 a_2=475.8, b_2=0.01808,c_2=1.246 a_3=110.7, b_3=0.07156, c_3=0.9868 a_4=97.37, b_4=0.06933, c_4=−1.933 a_5=5.184, b_5=0.1332, c_5=0.2161
Light-Green	$r(g) = \begin{cases} Red \\ \sum_{k=1}^{5} a_k \cdot sin(b_k g + c_k) \end{cases}$	a_1=385.5,b_1=0.009698,c_1=−0.1909 a_2=222, b_2=0.01261,c_2=2.775 a_3=6.941, b_3=0.05087, c_3=1.198 a_4=5.126, b_4=0.05422, c_4=3.995 a_5=0.05556, b_5=0.1116, c_5=−0.439
	Green $g(g) = \sum_{k=1}^{5} a_k \cdot sin(b_k g + c_k)$	a_1=645.5,b_1=0.009626,c_1=0.01047 a_2=428.4, b_2=0.0111,c_2=3.084 a_3=6.55, b_3=0.0643, c_3=−2.701 a_4=5.569, b_4=0.06904, c_4=−0.08461 a_5=0.3554, b_5=0.114, c_5=−1.629
	Blue $b(g) = \sum_{k=1}^{5} a_k \cdot sin(b_k g + c_k)$	a_1=293.8,b_1=0.0107,c_1=−0.178 a_2=166.2, b_2=0.01612,c_2=2.746 a_3=24.42, b_3=0.01839, c_3=5.849 a_4=10.02, b_4=0.07467, c_4=1 a_5=9.035, b_5=0.0788, c_5=3.823

and significantly improves breast lesion visibility without excessively brightening already luminous areas.

In Figure 3, we highlight the performance of deep learning-based methods, BBCNN and IE-CGAN, alongside our proposed method, in scenarios with low-level details critical for

International Journal of Advances in Engineering and Management (IJAEM)
Volume 7, Issue 05 May 2025, pp: 471-482 www.ijaem.net ISSN: 2395-5252

applications like autonomous driving. BBCNN tends to retain global consistency but again struggles to enhance crucial local features necessary for object detection tasks, often resulting in details being indistinguishable. IE-CGAN provides a noticeable improvement by amplifying local contrasts but occasionally over-enhances brighter regions, thus potentially reducing the clarity of critical structural edges. Our proposed method significantly improves the clarity of low-level details essential for object detection, particularly for autonomous driving applications. It robustly preserves structural edges, maintains optimal brightness levels, and effectively enhances the subtle details crucial for reliable object recognition and decision-making systems.

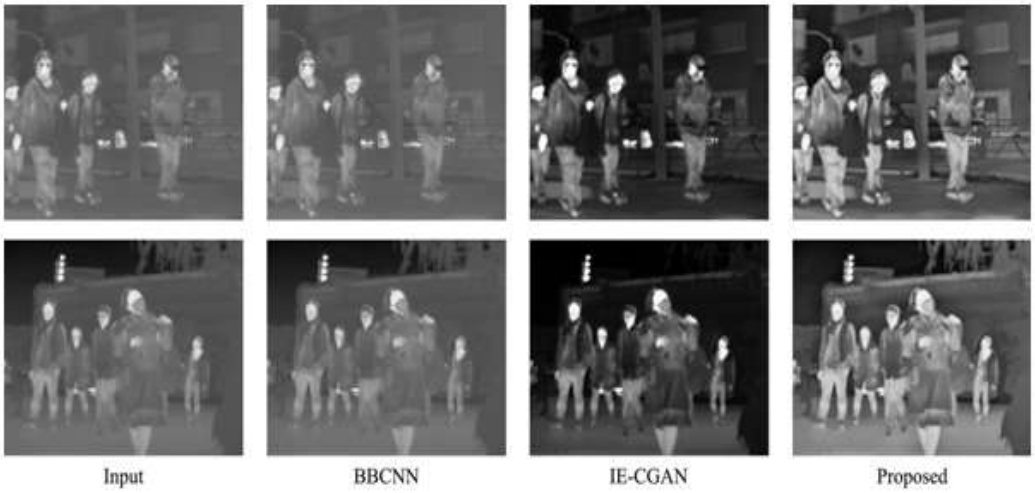

Figure 3. Qualitative comparison on the Autonomous vehicles dataset.

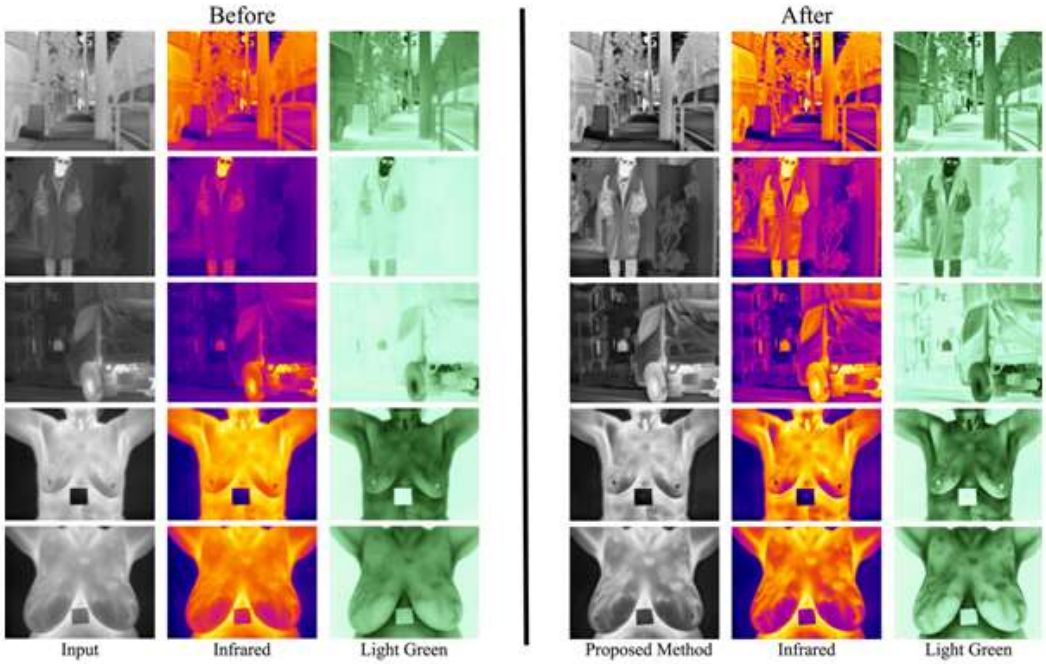

Figure 4. Colorization results before and after enhancement by the proposed method.

Figure 4 illustrates the transformative impact of pseudo-coloring after thermal enhancement. Before enhancement, thermal images present limited interpretability due to homogeneous brightness and a lack of distinct thermal differentiation. After enhancement, pseudo-coloring notably amplifies interpretability. Specifically, the infrared color scheme correctly highlights high-temperature regions, significantly improving visibility and aiding the quick

International Journal of Advances in Engineering and Management (IJAEM)
Volume 7, Issue 05 May 2025, pp: 471-482 www.ijaem.net ISSN: 2395-5252

identification of breast lesions and other temperature-critical anomalies. Conversely, the light-green palette provides enhanced visual comfort, making images more interpretable for continuous monitoring and extended analysis.

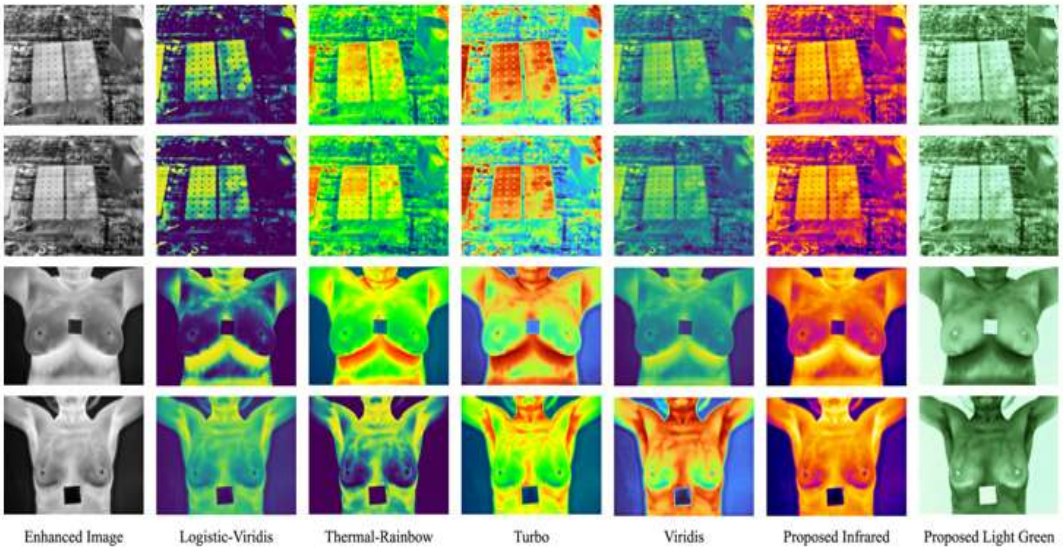

Figure 5. Qualitative comparison of the proposed method against another colorization method.

Figure 5 evaluates our proposed pseudo-coloring techniques against conventional colormaps (Logistic-Viridis, Thermal-Rainbow, Turbo, and Viridis), each computed using their default parameters. Standard colormaps, while visually appealing, present notable interpretation challenges. Logistic-Viridis and Viridis, despite their perceptual uniformity, often lack dynamic range, inadequately differentiating minor thermal variations critical in medical imaging and solar panel diagnostics. Thermal-Rainbow, although intuitive due to its color progression, still suffers from reduced perceptual uniformity and occasionally misleading abrupt hue transitions. The Turbo colormap, offering an improved luminance progression compared to traditional rainbow schemes, still occasionally introduces misleading categorical boundaries, particularly around the green-yellow transition. Our proposed infrared and light-green palettes comprehensively address these limitations. The infrared method distinctly enhances anomalies due to its strong contrast and intuitive "hot-cold" visual cues, significantly aiding in rapid anomaly detection. The light-green method provides excellent visual interpretability and user comfort, critical for prolonged analysis sessions and continuous real-time monitoring. The results highlight that our proposed method effectively combines superior enhancement performance with robust, interpretable pseudo-coloring techniques. It is highly suitable for practical deployment in diverse thermal imaging applications, including solar panel fault detection and autonomous driving systems.

Furthermore, as illustrated in Figure 6, numerous objects remain undetected in the original thermal video; however, after applying our enhancement, the detection results significantly improve.

QUANTITATIVE COMPARISON

To evaluate the effectiveness of the proposed method, we utilize three image quality metrics:

(i) The Measure of Enhancement (EME) [28] measures the contrast based on modified Weber's law, which is defined as the average of the local maximum and minimum grayscale intensities ratio in each sub-block.

$$EME(I) = \frac{1}{M \times N}\sum_{i=1}^{M}\sum_{j=1}^{N} 20\ log\frac{[I_{max}]_{i,j}^{m,n}}{[I_{min}]_{i,j}^{m,n} + c} \#(3)$$

where $[I_{min}]_{i,j}^{m,n}$ and $[I_{max}]_{i,j}^{m,n}$ denote the local minimum and maximum intensity level in each $m \times n$ local block. c represents a constant to avoid calculation errors due to a logarithmic operation.

In this metric, the image is divided into n blocks, where I_{max}^{k}, I_{min}^{k} represent the maximum and minimum pixel intensities within the k blocks, respectively. A small constant c is included to prevent division by zero [29].

(ii) Block Distribution-Based Information Measure (BDIM) [30] is a thermal image quality metric

International Journal of Advances in Engineering and Management (IJAEM)
Volume 7, Issue 05 May 2025, pp: 471-482 www.ijaem.net ISSN: 2395-5252

based on Human Visual System (HVS) attributes such as local resolution, contrast, and sharpness.

$$BDIM(p,I) = \frac{1}{M \times N}\sum_{i=1}^{M}\sum_{j=1}^{N}\frac{1}{\left(\frac{p_{min}^{m,n}}{p_{min}^{m,n}+p_{max}^{m,n}}\right)\left(\frac{(I_{min})_{i,j}^{m,n}}{(I_{min})_{i,j}^{m,n}+(I_{max})_{i,j}^{m,n}}\right)^2 + c} \quad \#(4)$$

where p_{min} and p_{max} respectively denote the minimum probability density value and the maximum probability density value in each local tile $[m,n]$, $(I_{min})_{i,j}^{m,n}$ and $(I_{max})_{i,j}^{m,n}$ represent the minimum intensity value and the maximum intensity value in each local tile $[m,n]$, respectively, and c refers to an offset value [29].

(iii) The Global Contrast Measure of Enhancement (MDIMTE) [31] integrates principles from the human visual system, information theory, and distribution-based analysis to assess enhancement quality. This metric offers a comprehensive evaluation by capturing global contrast improvements in a manner that aligns with human perception and reflects the efficiency of information distribution across the image.

Table 2. Quantitative comparison of the proposed method against other methods.

Datasets	Methods	EME↑	BDIM↑	MDIMTE↑	LGTA↑
Autonomous Vehicles	AGCWD	2.21	0.92	49.35	1.141
	AGCCPF	2.54	0.94	53.15	1.252
	BBCNN	2.19	0.94	53.82	1.180
	IE-CGAN	6.15	0.95	46.27	1.189
	Proposed	**9.18**	**0.96**	**54.12**	**1.312**
SOLAR	AGCWD	2.10	0.91	51.48	1.101
	AGCCPF	2.34	0.94	54.23	1.284
	BBCNN	3.30	0.95	54.98	1.191
	IE-CGAN	6.33	0.95	48.12	1.239
	Proposed	**10.80**	**0.97**	**55.89**	**1.352**
BREAST	AGCWD	4.27	0.93	48.14	1.014
	AGCCPF	4.05	0.94	52.16	1.124
	BBCNN	4.45	0.94	53.52	1.191
	IE-CGAN	11.20	0.95	45.27	1.212
	Proposed	**11.74**	**0.96**	**53.91**	**1.287**

$$MDIMTE(I) = \frac{1}{M \times N}\sum_{i=1}^{M}\sum_{j=1}^{N}\frac{(p_D)_{i,j}^{m,n}}{(p_B)_{i,j}^{m,n}}\left(\frac{(I_D)_{i,j}^{m,n}}{(I_B)_{i,j}^{m,n}}\right)^2 \quad \#(5)$$

where $(I_D)_{i,j}^{m,n}$ and $(I_B)_{i,j}^{m,n}$ represent the local darkness and brightness intensity level, respectively, and where $(p_D)_{i,j}^{m,n}$ and $(p_B)_{i,j}^{m,n}$ are the local darkness and brightness density in each $m \times n$ local block [29].

(iv) Local and Global Thermal Assessment (LGTA) [29], which integrates local and global features to evaluate thermal image quality comprehensively. Combining block-level analysis with global intensity distribution closely aligns with human perception, offering nuanced insights into image clarity and enhancement. The local thermal quality metric is determined by dividing the image into $k \times k$ blocks, then equations presented below are applied to these blocks using block-dependent local mean thresholds.

$$a' = \left(\frac{(max(I_L))^{m,n}+1}{(min(I_L))^{m,n}+2}\right)^{\beta};\ I_L = \{I_{i,j} | I_{i,j} \le x_\mu\}$$

$$a_{m,n} = a' cos(log(log\, a' + 1) + 1) \quad \#(6)$$

$$b' = \left(\frac{(max(I_U))^{m,n}+1}{(min(I_U))^{m,n}+2}\right)^{\beta};\ I_U = \{I_{i,j} | I_{i,j} \le x_\mu\}$$

$$b_{m,n} = b' cos(log(log\, b' + 1) + 1) \#(7)$$

where x_μ is the mean pixel value of the (m,n) block, β is a parameter (for example, β = 1, β> 1 or β< 1), and $max()(min)$ function calculates the block's third maximum (minimum) value if possible. The Local Thermal Assessment (LTA) is then computed:

International Journal of Advances in Engineering and Management (IJAEM)
Volume 7, Issue 05 May 2025, pp: 471-482 www.ijaem.net ISSN: 2395-5252

$$LTA(I) = \frac{1}{M \times N}\sum_{i=1}^{M}\sum_{j=1}^{N}\left(a_{m,n} + b_{m,n}\right) \#(8)$$

Table 3. Detection performance (mAP) on various inputs and models.

Measure	Original Images	Proposed Method
$mAP_{0.5}$	48.2	**50.8**
$mAP_{0.75}$	16.3	**18.5**
$mAP_{0.5:0.95}$	22.5	**24.1**

Capturing local variations and subtle details is crucial for accurate quality assessment in thermal image analysis. Traditional global metrics often overlook these nuances, leading to potentially misleading evaluations. To address this, they introduce the LTA metric, designed to provide a fine-grained image quality assessment by focusing on local image characteristics. The Global Thermal Assessment (GTA) quality metric is calculated as follows:

Figure 3. Object detection performance on real-world road video before and after enhancement.

$$NS = \frac{std(I_S)}{(1 + |std(I_S) - std(I)|)} \#(9)$$

International Journal of Advances in Engineering and Management (IJAEM)
Volume 7, Issue 05 May 2025, pp: 471-482 www.ijaem.net ISSN: 2395-5252

$$GTA = \frac{NS}{\sum_{i=1}^{M}\sum_{j=1}^{N} \quad log\left(log\left(\frac{p_{i,j}}{p_i \cdot p_j}+1\right)+1\right)} \#(10)$$

where p_i , p_j , and $p_{i,j}$ are the pixel's probability mass function (PMF) values in the current row, column, and whole image, respectively. The NS quantifies the noise level in the image, where $std(I_S)$ represents the standard deviation of the smoothed image I_S , and $std(I)$ represents the standard deviation of the original image I. The GTA measure comprehensively evaluates image quality by integrating 2D image histograms with column-wise and row-wise histograms. The 2D histogram captures the overall intensity distribution, while the column-wise and row-wise histograms reveal spatial variations, enabling a deeper understanding of image quality by considering global characteristics. This method is robust against spatial shifts and rotations—common challenges in image analysis—because it incorporates column-wise and row-wise histograms, which reduce the sensitivity of traditional 2D histograms to such transformations. GTA's enhanced sensitivity to specific image degradations, such as blur, noise, and contrast distortions, is particularly valuable for thermal imaging, which often presents unique image characteristics and degradations. To incorporate the local and global features of the thermal image, they define a combined Local and Global Thermal Assessment (LGTA) metric as a linear combination of LTA and GTA.

$$\mathrm{LGTA} = 0.5 \cdot \mathrm{LTA} + 0.5 \cdot \mathrm{GTA} \#(11)$$

High scores across these metrics reflect superior image enhancement and a more natural visual appearance. Table 2 presents the comparative analysis results, highlighting the proposed method's performance relative to existing approaches. The proposed method consistently outperforms traditional and learning-based techniques, achieving the highest average scores in EME, BDIM, MDIMTE, and LGTA. These findings underscore the effectiveness of the proposed framework in enhancing thermal images while preserving critical structural details and maintaining perceptual naturalness.

To further demonstrate the practical effectiveness of the proposed framework, we conducted a series of object detection experiments using YOLOv7. This evaluation is particularly relevant to autonomous driving scenarios, where accurate and robust object detection under varying thermal conditions is essential for ensuring safety and operational reliability. Separate YOLOv7 models were trained using default hyperparameters on the colorized far-infrared images from the Autonomous Vehicles dataset [25], with two configurations: original thermal images and images enhanced by the proposed method.

For quantitative evaluation, we employed standard object detection metrics, including mean Average Precision at a 50% Intersection over Union (IoU) threshold ($mAP_{0.5}$), mean AP at a 75% IoU threshold ($mAP_{0.75}$), and the average AP across IoU thresholds from 0.5 to 0.95 ($mAP_{0.5:0.95}$).

Table 3 summarizes the detection results under each experimental setting. The findings indicate that all enhanced image variants yielded superior detection performance compared to their original counterparts. Notably, the proposed method achieved a 2.6% improvement in $mAP_{0.5}$, a 2.2% improvement in $mAP_{0.75}$, and a 1.6% gain in $mAP_{0.5:0.95}$, underscoring its practical utility for real-world applications such as autonomous vehicle perception.

Table 4. Ablation study using Detection on colorized and enhanced images

Measure	Enhanced	Colorized
$mAP_{0.5}$	50.1	**50.8**
$mAP_{0.75}$	17.8	**18.5**
$mAP_{0.5:0.95}$	23.4	**24.1**

IV. ABLATION STUDY

We conducted a series of ablation experiments to assess the contribution of the colorization process to the object detection performance. Specifically, we trained the object detection network with and without the colorized images after enhancement. Table 4 shows that accuracy significantly improved when the detection was trained with colorful images using $mAP_{0.5}$, $mAP_{0.75,}$ and $mAP_{0.5:0.95}$ measures. This further highlights the importance of colorizing methods in downstream tasks such as Autonomous Driving systems.

V. CONCLUSION

This paper introduces a unified pipeline for thermal image enhancement, effectively addressing limitations such as low contrast and indistinct details that impede human interpretation and automated analysis. Our approach significantly improves visual clarity and preserves crucial structural information by systematically combining decomposition, illumination balancing, and a pseudo-coloring scheme. Extensive experiments on diverse benchmark datasets show that our method consistently outperforms existing techniques. Enhanced images produced by the proposed pipeline deliver superior visual quality and preserve fine details, improving performance in automated object detection tasks.

Building on these promising results, future research will focus on refining the pipeline further. This involves exploring advanced techniques or adaptive parameterization for its core stages. Optimizing for deployment on resource-constrained edge devices remains a priority to enhance its utility in real-time systems prevalent in autonomous driving and portable diagnostics. Finally, a significant avenue for exploration is how these enhanced images can serve as superior input for training more complex deep learning models, potentially improving performance in tasks such as semantic segmentation or anomaly detection in thermal imagery.

REFERENCES

[1]. X. Zhong, T. Lu, W. Huang, M. Ye, X. Jia and C.-W. Lin, "Grayscale enhancement colorization network for visible-infrared person re-identification," IEEE Transactions on Circuits and Systems for Video Technology, vol. 32, no. 3, pp. 1418--1430, 2021.

[2]. N. O. Alsrehin, A. F. Klaib and A. Magableh, "Intelligent transportation and control systems using data mining and machine learning techniques: A comprehensive study," IEEE Access, vol. 7, pp. 49830--49857, 2019.

[3]. G. F. Shidik, E. Noersasongko, A. Nugraha, P. N. Andono, J. Jumanto and E. J. Kusuma, "A systematic review of intelligence video surveillance: Trends, techniques, frameworks, and datasets," IEEE Access, vol. 7, pp. 170457--170473, 2019.

[4]. T. Trongtirakul, S. Agaian and A. Oulefki, "Automated tumor segmentation in thermographic breast images," Mathematical Biosciences and Engineering, vol. 20, no. 9, pp. 16786--16806, 2023.

[5]. H.-T. Wu, X. Cao, R. Jia and Y.-M. Cheung, "Reversible data hiding with brightness preserving contrast enhancement by two-dimensional histogram modification," IEEE Transactions on Circuits and Systems for Video Technology, vol. 32, no. 11, pp. 7605--7617, 2022.

[6]. C. Liu, X. Sui, X. Kuang, Y. Liu, G. Gu and Q. Chen, "Adaptive contrast enhancement for infrared images based on the neighborhood conditional histogram," Remote sensing, vol. 11, no. 11, p. 1381, 2019.

[7]. A. M. Reza, "Realization of the contrast limited adaptive histogram equalization (CLAHE) for real-time image enhancement," Journal of VLSI signal processing systems for signal, image and video technology, vol. 38, pp. 35--44, 2004.

[8]. T. Mudavath and V. Niranjan, "Thermal image enhancement for adverse weather scenarios: a wavelet transform and histogram clipping approach," Signal, Image and Video Processing, vol. 18, no. 10, pp. 6547--6558, 2024.

[9]. C. Dong, C. C. Loy, K. He and X. Tang, "Image super-resolution using deep convolutional networks," IEEE transactions on pattern analysis and machine intelligence, vol. 38, no. 2, pp. 295--307, 2015.

[10]. J. Kim, J. K. Lee and K. M. Lee, "Accurate image super-resolution using very deep convolutional networks," in Proceedings of the IEEE conference on computer vision and pattern recognition, 2016.

[11]. M. A. Marnissi, "Revolutionizing thermal imaging: GAN-based vision transformers for image enhancement," in IEEE International Conference on Image Processing (ICIP), 2023.

[12]. Z. Shen, F. Qin, R. Ge, C. Wang, K. Zhang and J. Huang, "IDTransformer: Infrared image denoising method based on convolutional transposed self-attention," Alexandria Engineering Journal, vol. 110, pp. 310--321, 2025.

[13]. X. Kuang, X. Sui, Y. Liu, Q. Chen and G. Gu, "Single infrared image enhancement using a deep convolutional neural network," Neurocomputing, vol. 332, pp. 119--128, 2019.

[14]. B. Zhan and Y. Wu, "Infrared image enhancement based on wavelet transformation and retinex," in Second International Conference on Intelligent

Human-Machine Systems and Cybernetics, 2010.
[15]. K. Lee, J. Lee, J. Lee, S. Hwang and S. Lee, "Brightness-based convolutional neural network for thermal image enhancement," Ieee Access, vol. 5, pp. 26867--26879, 2017.
[16]. S. Rahman, M. M. Rahman, M. Abdullah-Al-Wadud, G. D. Al-Quaderi and M. Shoyaib, "An adaptive gamma correction for image enhancement," EURASIP Journal on Image and Video Processing, pp. 1--13, 2016.
[17]. D. Oladepo, C. McCausland, R. Bond, D. Finlay and P. Biglarbeigi, "Color by Numbers: The Implications of Colormap Selection in Deep Learning's Perception," Information Sciences, p. 121889, 2025.
[18]. R. M. Karim, O.-H. Kwon, C. Park and K. Lee, "A study of colormaps in network visualization," Applied Sciences, vol. 9, no. 20, p. 4228, 2019.
[19]. A. Mikhailov, "Turbo, An Improved Rainbow Colormap for Visualization," Google Research, aug 20 2019. [Online]. Available: https://research.google/blog/turbo-an-improved-rainbow-colormap-for-visualization/. [Accessed 17 May 2025].
[20]. O. Alpar, "Nakagami imaging with related distributions for advanced thermogram pseudocolorization," Journal of Thermal Biology, vol. 93, p. 102704, 2020.
[21]. C. Ware, M. Stone and D. A. Szafir, "Rainbow colormaps are not all bad," IEEE Computer Graphics and Applications, vol. 43, no. 3, pp. 88--93, 2023.
[22]. W. Wu, J. Weng, P. Zhang, X. Wang, W. Yang and J. Jiang, "Uretinex-net: Retinex-based deep unfolding network for low-light image enhancement," in Proceedings of the IEEE/CVF conference on computer vision and pattern recognition, 2022.
[23]. Y. Zhang, K. Li, K. Li, L. Wang, B. Zhong and Y. Fu, "Image super-resolution using very deep residual channel attention networks," in Proceedings of the European conference on computer vision (ECCV), 2018.
[24]. C.-Y. Wang, A. Bochkovskiy and H.-Y. M. Liao, "YOLOv7: Trainable bag-of-freebies sets new state-of-the-art for real-time object detectors," in Proceedings of the IEEE/CVF conference on computer vision and pattern recognition, 2023.
[25]. K. Takumi, K. Watanabe, Q. Ha, A. Tejero-De-Pablos, Y. Ushiku and T. Harada, "Multispectral object detection for autonomous vehicles," in Proceedings of the on Thematic Workshops of ACM Multimedia 2017, 2017.
[26]. E. Alfaro-Mej´ıa, "Dataset for recognition of snail trails and hot spot failures in monocrystalline Si solar panels," Data in brief, vol. 26, p. 104441, 2019.
[27]. L. Silva, D. Saade, G. Sequeiros, A. Silva, A. Paiva, R. d. S. Bravo and A. Conci, "Journal of Medical Imaging and Health Informatics," A new database for breast research with infrared image, vol. 4, no. 1, pp. 92--100, 2014.
[28]. S. S. Agaian, K. Panetta and A. M. Grigoryan, "A new measure of image enhancement," in IASTED International Conference on Signal Processing & Communication, 2000.
[29]. S. Agaian, H. Ayunts, T. Trongtirakul and S. Hovhannisyan, "A new method for judging thermal image quality with applications," Signal Processing, vol. 229, p. 109769, 2025.
[30]. T. Trongtirakul and S. Agaian, "Unsupervised and optimized thermal image quality enhancement and visual surveillance applications," Signal Processing: Image Communication, vol. 105, p. 116714, 2022.
[31]. S. Agaian, M. Roopaei and D. Akopian, "Thermal-image quality measurements," in IEEE international conference on acoustics, speech and signal processing (ICASSP), 2014.